TSINGHUA SCIENCE AND TECHNOLOGY
ISSNll1007-0214 09/10 pp615–629
DOI: 10.26599/TST.2018.9010091
Volume 24, Number 5, October 2019

WiSH: WiFi-Based Real-Time Human Detection

Tianmeng Hang, Yue Zheng, Kun Qian, Chenshu Wu, Zheng Yang*, Xiancun Zhou, Yunhao Liu, and Guilin Chen

Abstract: Sensorless sensing using wireless signals has been rapidly conceptualized and developed recently. Among numerous applications of WiFi-based sensing, human presence detection acts as a primary and fundamental function to boost applications in practice. Many complicated approaches have been proposed to achieve high detection accuracy, but they frequently omit various practical constraints such as real-time capability, computation efficiency, sampling rates, deployment efforts, etc. A practical detection system that works in real-world applications is lacking. In this paper, we design and implement WiSH, a real-time system for contactless human detection that is applicable for whole-day usage. WiSH employs lightweight yet effective methods and thus enables detection under practical conditions even on resource-limited devices with low signal sampling rates. We deploy WiSH on commodity desktops and customized tiny nodes in different everyday scenarios. The experimental results demonstrate the superior performance of WiSH, which has a detection accuracy of >98% using a sampling rate of 20 Hz with an average detection delay of merely 1.5 s. Thus, we believe WiSH is a promising system for real-world deployment.

Key words: channel state information; human detection; real-time system; wireless sensing; off-the-shelf WiFi

1 Introduction

Wireless signals play an important role in our daily lives. In the past, such signals were usually used as a sole communication medium. Nowadays, they appear more frequently in the sensing area[1]. Sensorless sensing has been quickly developed and enriched from both theoretical foundations and innovative applications. Received Signal Strength Indicator (RSSI) has been adopted in indoor localization systems. However, in complex situations, it suffers from dramatic performance degradation because of multipath fading and temporal dynamics. Channel State Information (CSI) is able to discriminate multipath characteristics and help analyze and capture human motions. A number of motivating applications have been enabled or improved, such as human detection[2,3], human activity monitoring[4], gesture recognition and interaction[5], gait recognition[6], smoking detection[7], keystroke recognition[8], sleep monitoring[9], fall detection[10], and respiration and heart rate monitoring[11], etc. While many researchers continue to foster more attractive applications with complicated designs, we argue that building and

• Tianmeng Hang, Yue Zheng, Kun Qian, Zheng Yang, and Yunhao Liu are with the School of Software and BNRist, Tsinghua University, Beijing 100084, China. E-mail: {hangtianmenglisa, cczhengy, qiank10, hmilyyz, yunhaoliu}@gmail.com.
• Yunhao Liu is also with the Department of Computer Science and Engineering, Michigan State Unversity, East Lansing, MI 48824, USA.
• Chenshu Wu is with the Department of Electrical & Computer Engineering, Univeristy of Maryland, College Park, MD 20742, USA. E-mail: wucs32@gmail.com.
• Xiancun Zhou is with the School of Information Engineering, West Anhui University, Lu'an 237012, China. E-mail: zhouxcun@mail.ustc.edu.cn.
• Guilin Chen is with the School of Computer and Information Engineering, Chuzhou University, Chuzhou 239000, China. E-mail: glchen@chzu.edu.cn.
† Tianmeng Hang and Yue Zheng contribute equally to this paper.
* To whom correspondence should be addressed.
Manuscript received: 2018-01-12; revised: 2018-03-04; accepted: 2018-03-10

validating simple and effective sensing systems that are applicable in practice are of equal importance and value to the community.

As dedicated or wearable sensors are too heavy for daily lives, many systems have proposed to enable various human sensing applications without using them. However, strict requisites must be followed if sensing systems are deployed in real environments. For example, dense links are required for accurate localization and tracking[12]. Sleep monitoring systems ask users to be very close to the wireless links for sleep monitoring[9]. These systems may employ extensive prior training for different locations for keystroke or activity recognition[4, 8, 13]. A truly practical wireless human sensing system that functions in the real-world applications is lacking. In this paper, we aim to design and implement a real-time system of contactless human detection, which works in practice for whole-day usage yet does not resort to impractical conditions such as dense links, location-dependent prior trainings, or interference-free environments.

Human detection, a primary and fundamental function among plentiful applications, appears to be one of the most practically applicable killer applications, which is promising for real-world deployment. Knowledge of human presence is a valuable primitive for security monitoring, smart home monitoring, exhibition interaction, mall analytics, and factory environment control. Effective approaches have been proposed for human detection[2, 3, 14]. However, these methods suffer from several limitations for real-time applications. Typically, they require prior training and high sampling rates, and employ complex algorithms, rendering them infeasible for energy-efficient and real-time applications. In addition, most existing systems are designed for arbitrary motion sensing that perceives any locomotion instead of exact human detection, which targets human presence events.

In this paper, we present WiSH, a lightweight system for real-time *Wireless Sensing of Human* detection. To boost applications in practice, WiSH employs an efficient detection algorithm that works with one single pair of transmitter and receiver and extremely low sampling rates. Specifically, we extract simple but effective features from both time and frequency correlations of the received WiFi signals. On this basis, we design a robust event filter to deal with mis-alarms induced by instantaneous eruptions due to uncertain environmental dynamics. The key insight is that human presence events usually last for a certain duration. Thanks to its effectiveness and robustness, WiSH is widely applicable for whole-day deployment in different practical scenarios.

We implement WiSH on two types of devices: commodity desktops and laptops and customized embedded nodes, as shown in Fig. 1. The desktops are commodity mini PCs, whereas the customized nodes are tiny programmable routers that also support CSI measurement yet with limited computing resource. The tiny device is energy efficient, portable, easy to deploy, and most importantly, inexpensive at about $10. A real-time system applicable on such nodes can be easily installed and is promising for practical everyday usage. WiSH executes the complete detection procedure as a standalone algorithm on end devices independently and announces detection events locally or outputs the detection results to a central server in real time, which then visualizes the detected events.

To evaluate the performance of WiSH, we deploy it in different scenarios such as laboratory offices, classrooms, and home environments. We install a vision-based system to obtain the ground truths. We collect data for over 72 hours, which consists of over 300 movement events. Results demonstrate that WiSH achieves grateful detection performance even with a low sampling rate of 20 Hz on resource-limited devices. Specifically, WiSH yields a detection accuracy of >98%. The average detection delay is 1.5 s, whereas

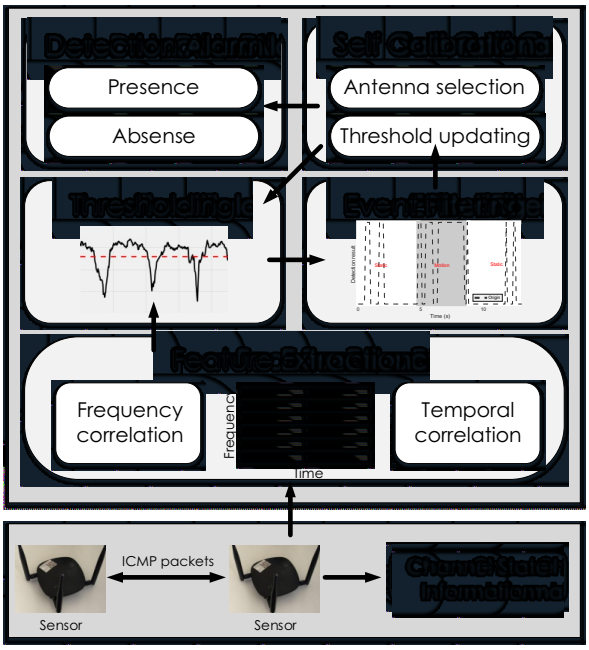

Fig. 1 Framework of WiSH.

the durations of all detected events overlap with true events by 76.7%, which grows to 92.5% if the sampling rate increases to 90 Hz.

In summary, our core contributions are as follows:

• We present WiSH, a real-time system for contactless human detection for whole-day usage. The design of WiSH fully accounts for various practical constraints including accuracy, detection delays, computation complexity, and signal sampling rate, and thus renders WiSH applicable for real-world deployment.

• We propose a lightweight method that harnesses both frequency and time correlations for motion sensing and employs a robust event filter for human detection, which enables effective human presence event detection even on resource-limited but easy-to-deploy devices with low CSI sampling rates.

• We implement and deploy WiSH on commodity PCs and customized cheap and portable devices. The results demonstrate the promising applicability of WiSH for practical daily monitoring.

The rest of the paper is organized as follows. We describe the design goals in Section 2. The algorithms are presented in Section 3. System implementation and evaluation are provided in Sections 4 and 5, respectively. We review the literature in Section 6 and conclude this paper in Section 7.

2 Design Space

2.1 Application scenarios

Human detection is a long-standing and valuable problem that has attracted numerous efforts from both academic and industrial sides. Compared with previous detection manners such as infra-red or vision-based approaches, WiFi-based systems have advantages in low costs, omni-directional coverage, through-wall capabilities, and privacy-preserving features. Hence, WiFi-based sensorless sensing is useful in various applications.

Typically, wireless human detection can be used for intruder detection for home security, storehouse monitoring, and hotel services. Take hotels as an example. A waiter should not disturb the customers if they are detected to be in the room via a privacy-friendly manner. Sleep monitoring can also benefit a lot from sensorless sensing. The experience will be largely enhanced if light can be intelligently turned on/off with a system that automatically senses a person getting up at night to urinate. Wireless sensing is also helpful to smart home and smart building analytics. By analyzing the presence durations and patterns of a user at home, building architects can improve the indoor space design. As a primitive, all these applications demand a practical and easy-to-deploy system that is capable of whole-day detection of human presence in real time.

2.2 Design goals

We expect WiSH to be a practical human detection system for whole-day monitoring. To achieve this goal, the system should meet the following properties.

• Accurate and robust. WiSH should accurately detect human presence events, yet reduce false alarms to the minimum extent.

• Real-time. WiSH should detect and report human presence events in real time. Delay-sensitive applications such as intruder detection may require instantaneous results for emergency responses.

• Energy efficient. We envision the capability of human sensing to be integrated in general communication devices or installed on battery-powered devices in the future. Thus, energy consumption, either by CSI sampling or computation, should be as low as possible.

• Low sampling rate. WiSH works on communication devices in a non-invasive manner. To restrict the influence on communication, a detection system should yield reasonable accuracy with low sampling rates.

Most existing systems achieve good performance but rely on extremely high sampling rates (e.g., 100 Hz to 1000 Hz[2, 15]) and do not work in real time. In this paper, we design and implement WiSH, which is expected to be capable of real-time detection for whole-day applications. In contrast to mainly considering detection precision, WiSH targets real-world applicability and fully accounts for various practical constraints including real-time capability, energy efficiency, sampling rate limitation, computation complexity, and deployment efforts.

3 Methods

3.1 System flow

WiSH is a system that utilizes CSI to implement human detection. CSI depicts channel properties of a wireless link and is provided by off-the-shelf Network Interface Cards (NICs) with slight driver modification. In static/dynamic environments, CSI exhibits different characteristics. Thus, CSI is a favorable indicator of a

moving human with proper features extracted. As we aim to implement real-time human detection, latency, computational cost, and energy cost should also be considered when designing features. How to propose a lightweight detection algorithm is the first challenge we need to undertake. Furthermore, due to the presence of noise and radio frequency interference, CSI might be unstable even without moving targets. False alarms will arise if we cannot filter the exceptional events. Therefore, the second challenge is to implement a robust event filter on the basis of the observation that dynamic changes in the propagation environment induced by humans usually lasts for a sufficiently long duration. We find that different antennas of the receiver might suffer various degrees of dynamics when a person is walking. And channel properties might vary even if the surroundings slightly change. In order to promote the robustness and sensitiveness of the system, a suitable self-calibration mechanism must be adopted.

Figure 1 depicts the overall framework of WiSH. The system first retrieves CSI by exchanging Internet Control Message Protocol (ICMP) packets between sensors. The obtained CSI is then fed into the upper layer for further processing. First, features of correlation in both time and frequency domains are calculated. Subsequently, a threshold is applied to the features to preliminarily detect moving entities in the monitoring area. The preliminary noisy detection result is further filtered based on the limitation of the minimum length of moving event. With trustworthy ground truth obtained during a specific time such as midnight when there are likely no moving entities in the monitoring area, the system calibrates itself to select stable antennas and update the preliminary threshold. The system alarms once the output indicates the existence of moving entities.

3.2 Detection algorithm

With CSI Tool[16] deployed on commodity WiFi devices, CSI can be collected in the following format:

$$H = [H(f_1), H(f_2), \ldots, H(f_k), \ldots, H(f_N)]^{\mathrm{T}}, \quad k \in [1, N] \tag{1}$$

where N denotes the total number of subcarriers in an Orthogonal Frequency Division Multiplexing (OFDM) symbol, and f_k denotes the central frequency of the k-th subcarrier. $H(f_k)$ is defined as

$$H(f_k) = |H(f_k)| \mathrm{e}^{j \angle H(f_k)} \tag{2}$$

where $|H(f_k)|$ and $\angle H(f_k)$ denote the amplitude and phase, respectively. Raw phase information is usually random due to noise, packet boundary detection uncertainty, central frequency offset, and sampling frequency offset[17]. Thus, we only utilize the amplitude of CSI to detect movement events.

To implement the human detection algorithm, we first collect continuous CSI measurements over a sliding window W. Suppose that the sliding window consists of T CSI measurements under a specific sampling rate, then a matrix M in the time-frequency domain can be expressed as

$$M = [H_1, H_2, \ldots, H_i, \ldots, H_T] = [S_1^{\mathrm{T}}, S_2^{\mathrm{T}}, \ldots, S_j^{\mathrm{T}}, \ldots, S_F^{\mathrm{T}}]^{\mathrm{T}} \tag{3}$$

where H_i denotes the CSI collected at the i-th sampling time in the sliding window, and S_j denotes the CSI sequence of the j-th subcarrier.

The core idea of motion detection is to quantize variations of CSI. However, simply calculating variances of CSI suffers from hardware issues such as power control. Instead, we use correlation of CSI in both time and frequency domains to indicate the existence of movement events. Specifically, in the time domain, we calculate cross-correlation of each pair of CSI. Figure 2 shows the average cross-correlations of different CSI pairs in a sliding window. Intuitively, when the environment is static, all CSI measurements in the sliding window are highly correlated, with cross-

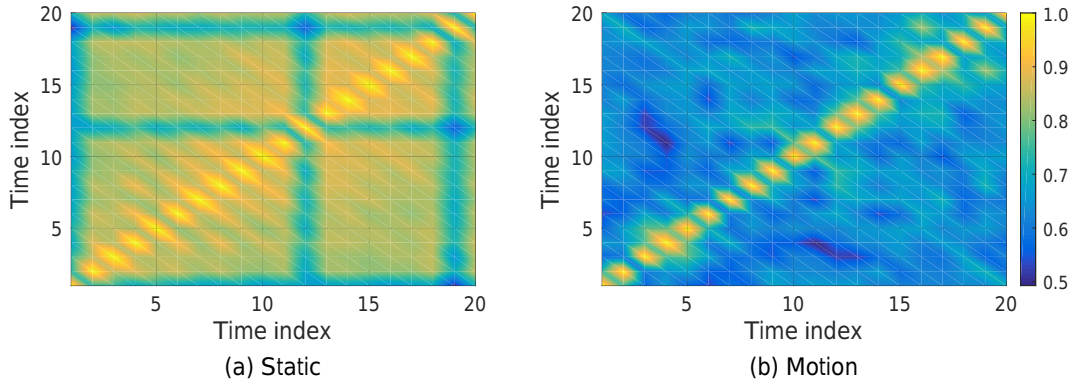

Fig. 2 Distribution of temporal correlation of CSI in (a) static cases and (b) motion cases.

correlation higher than 0.95. By contrast, when entities are moving in the environment, the cross-correlation between different CSI measurements significantly decreases to 0.8.

In addition to the time domain, we further study the correlating property of CSI in the frequency domain. Specifically, the cross-correlation of CSI sequences of different subcarriers is calculated. Figure 3 plots the distribution of cross-correlation in the frequency domain in the presence and absence of moving entities. The dot on each subcarrier bar means the median cross-correlation in frequency. Clearly, the existence of moving entities statistically decreases the cross-correlation of most subcarriers. However, the variation of frequency correlation is not as stable as that of time correlation.

To leverage cross-correlation in both time and frequency domains, we select median values of both correlation data, and integrate both correlations as Motion Indicator (MI):

$$\mathrm{MI} = \bar{c_t} \mathrm{e}^{0.1\bar{c_f}} \tag{4}$$

where $\bar{c_t}$ is the median time correlation, and $\bar{c_f}$ is the median frequency correlation. A coefficient of 0.1 and the exponential operator are used to accommodate the noisy fluctuation of frequency correlation. We employ training data to determine the most suitable coefficient. A threshold is applied for MI to preliminarily detect motion of entities in the monitor area. Note that movement events result in lower values of MI, and we regard such MIs as positive in this paper.

In particular, when we calculate cross-correlation in frequency, we do not have to calculate all the cross-correlations between every subcarrier. Instead, we randomly select some subcarriers from all subcarriers and only calculate their cross-correlation. With this method, operation time is largely shortened and overall performance is almost similar. The detection algorithm is detailed in Algorithm 1.

3.3 Robust event filter

WiFi operates in the free 2.4/5 GHz ISM band, which is exceedingly crowded especially in modern buildings. Apart from our own system, a great number of radio devices are also functioning and we can hardly find an interference-free channel. In order to resist interference, a WiFi receiver might adjust power to guarantee correct decoding. It might also change the modulation and coding scheme index when the communication quality of the channel degrades. Both of above result in the observation that CSI amplitude suffers abrupt fluctuations occasionally. False alarms will arise in

Algorithm 1 Motion indicator calculation

Input: M: $F \times T$ CSI matrix
Output: MI: Motion indicator

/* Calculate correlation of CSI samples*/
for all $t_1, t_2 = 1, \ldots, T$ **do**
$c_t(t_1, t_2) = \frac{H_{t_1}^{\mathrm{T}} H_{t_2}}{\|H_{t_1}\| \|H_{t_2}\|}$
end for
$\bar{c}_t = \mathrm{Median}(c_t(t_1, t_2))$

/* Calculate correlation of CSI subcarriers*/
Randomly pick a certain number of subcarriers from all subcarriers
for all $f_1, f_2 = 1, \ldots, F_{\mathrm{select}}$ **do**
$c_f(f_1, f_2) = \frac{S_{f_1} S_{f_2}^{\mathrm{T}}}{\|S_{f_1}\| \|S_{f_2}\|}$
end for
$\bar{c}_f = \mathrm{Median}(c_f(f_1, f_2))$

/* Calculate motion indicator */
$\mathrm{MI} = \bar{c}_t \mathrm{e}^{0.1\bar{c}_f}$

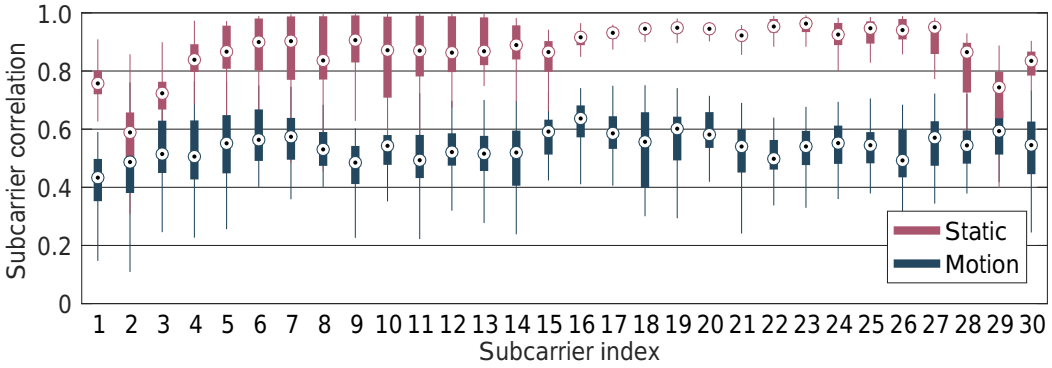

Fig. 3 Distribution of frequency correlation of CSI.

the event of a sufficient number of exceptional CSI measurements in the sliding window.

To decrease false alarms, we propose a robust event filter on the basis that human presence events usually last for a sufficiently long time. By contrast, eruptions induced by interference do not appear continuously. We formally illustrate how the event filter works in the following. Suppose that for sliding widow W_i, the corresponding motion indicator MI_i is determined to have a positive status. We then observe the following MIs continuously. Only when all the values in the sequence $\mathrm{MI}_i, \mathrm{MI}_{i+1}, \ldots, \mathrm{MI}_{i+d_1-1}$ are lower than the threshold will the system alarm the presence of moving entities (see Fig. 4a). Besides, as we adopt a fixed threshold for motion indicators, human movements might be ignored if the corresponding MIs fluctuate around the threshold. The phenomenon is not uncommon as the effects that human movements exert on CSI might degrade at specific locations. Therefore, as long as the interval between two positive motion indicators MI_j and MI_k is less than d_2, we regard the sequence $\mathrm{MI}_j, \mathrm{MI}_{j+1}, \ldots, \mathrm{MI}_k$ as positive (see Fig. 4b). The pseudocode is shown in Algorithm 2.

Algorithm 2 Principles of the event filter

Input:
MIS: $1 \times T$ Motion indicator sequence
ϵ: Threshold for motion indicator
d_1, d_2: Thresholds for event filter
Output: DS: $1 \times T$ Detection sequence

```
/* Detection with rough threshold */
for all t = 1, ..., T do
  DS_t = {MIS_t < ε}
end for

/* Filter false alarms of motion */
for Successive DS_{t,...,t+L+1} do
  if DS_t = 0 and DS_{t+L+1} = 0 then
    if DS_{t+1,...,t+L} = 1 and L < d_1 then
      DS_{t+1,...,t+L} = 0
    end if
  end if
end for

/* Filter static false alarms */
for Successive DS_{t,...,t+L+1} do
  if DS_t = 1 and DS_{t+L+1} = 1 then
    if DS_{t+1,...,t+L} = 0 and L < d_2 − 2 then
      DS_{t+1,...,t+L} = 1
    end if
  end if
end for
```

3.4 Self-calibration

For both detection algorithm and event filter, thresholds need to be determined preliminarily through training when the system is deployed. Considering that the environment settings might vary and channel properties also change, the value of thresholds might need to be recalibrated over a few days. A heuristic approach is to exploit the data collected after midnight (e.g., 3:00 a.m.–4:00 a.m.) for recalibration because moving entities are hardly present.

The performance of WiSH is also sensitive to antenna choice. As different antennas of the WiFi receiver correspond to different propagation environments, CSI collected by each antenna is distinct. Moreover, the dynamics of CSI induced by moving entities are at different degrees. Thus, the sensitivity of the antenna is crucial in detection accuracy. If the antenna is rather insensitive, then micro movements will be concealed. However, the performance will also degrade if the antenna is too sensitive. In such case, noise can be also regarded as movements and false alarms can arise. Therefore, improper antennas must be discarded. WiSH can automatically achieve antenna selection via

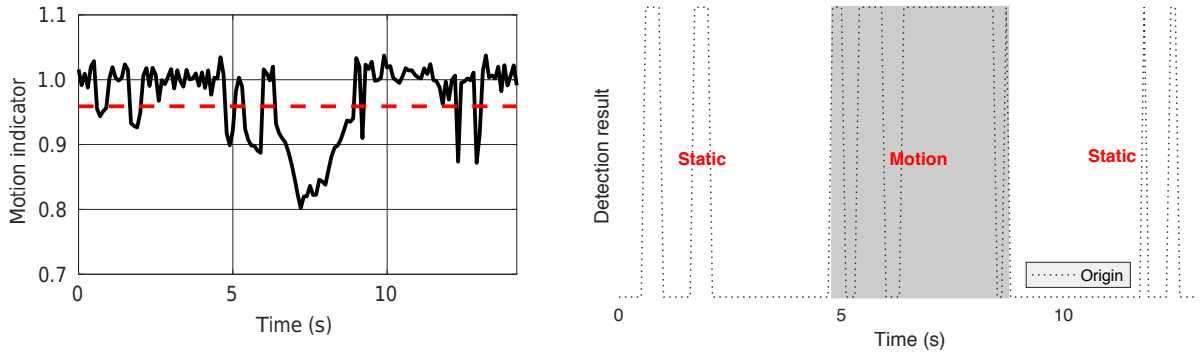

(a) Determine a movement event

(b) Splice adjacent movement events

Fig. 4 Examples of event filter.

detection accuracy comparison when recalibrating the thresholds.

4 Implementation

To deploy WiSH, we use two tiny WiFi nodes (shown in Fig. 5) as the transmitter and receiver. The node supports IEEE 802.11n standard, and we choose one channel in 2.4 GHz ISM band to operate WiSH. The transmitting node is equipped with one antenna, and the receiving node is equipped with three antennas. Thus, three groups of CSI which correspond to three individual wireless links are collected, and we splice them together to create a whole matrix as shown in Eq. (3). In contrast to traditional WiFi devices that are utilized to perform sensing applications (e.g, laptops and mini desktops), the node only uses 128 MB DDR2 RAM. In addition, the highest sampling rate is around 15 – 20 Hz because it is limited by hardware capability. This sampling rate is much lower than the used sampling rate of 100 – 1000 Hz in prior work[2, 6, 13].

However, the node exhibits the following favorable features. First, it is in low energy levels. In standby mode (WiFi turned off), the power is merely 462 MW. The power increases to 660 MW when there is a small communication flow. And the power in full load mode is 990 MW. Second, the cost of the node is only 10 dollars. Furthermore, the node is portable and easy to deploy. We use C language to implement the methodology and operate it in OpenWrt, which is an embedded operating system based on Linux. In order to exhibit real-time detection results, we also build a website that is depicted in Fig. 6. The red box indicates moving entities during this time duration.

Fig. 5 Tiny WiFi nodes.

To further investigate how the sampling rate affects the performance of the proposed methodology, we transfer the system to the traditional wireless platform. A TP-LINK TL-WDR7500 WiFi router that supports IEEE 802.11n standard functions as the transmitter, and a mini desktop (physical size 170 mm × 170 mm) with three antennas works as the receiver. The mini desktop is equipped with an Intel 5300 NIC and runs Ubuntu 12.04 OS. With Linux 802.11n CSI Tool deployed, the mini desktop can collect CSI measurements.

5 Evaluation

5.1 Experimental settings

Our experiments can be classified into two categories. First, to evaluate the performance of WiSH with tiny nodes deployed, we conduct experiments in a classroom, a meeting room, and a dormitory room. The classroom is 6 m × 10 m large, and the nodes are placed at the front of the classroom. In this case, we investigate how movement events at different locations, the distance between two nodes, the speed of the moving entity, and other factors affect the performance of WiSH. The effective covering range of WiSH can be determined via experiment results. The meeting room and dormitory room are 6 m × 3 m large and 3 m × 4 m large, respectively. WiSH is deployed in the above scenarios to monitor whether intrusion or moving events occur. The two tiny nodes are placed along the diagonal of the room. The transmitting node is 4 m away from the receiving node. Both are placed 1.2 m high. The floor plans are depicted in Fig. 7.

Second, given the limited hardware capacity of tiny nodes, we deploy the mini desktop and WiFi router in the classroom and meeting room to further investigate

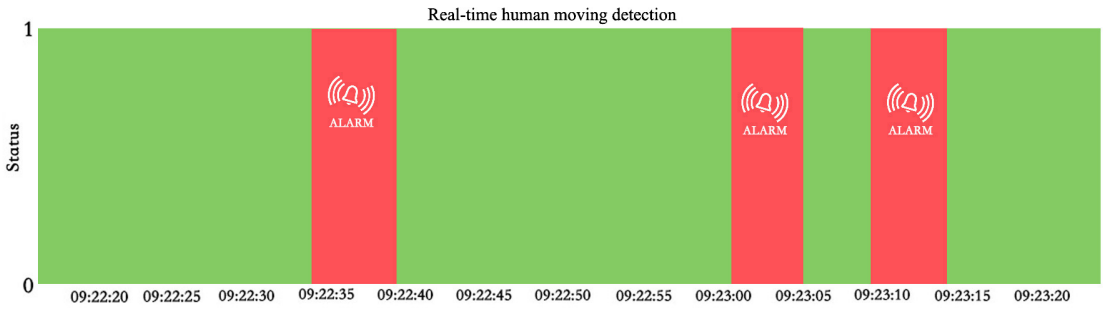

Fig. 6 Real-time GUI website.

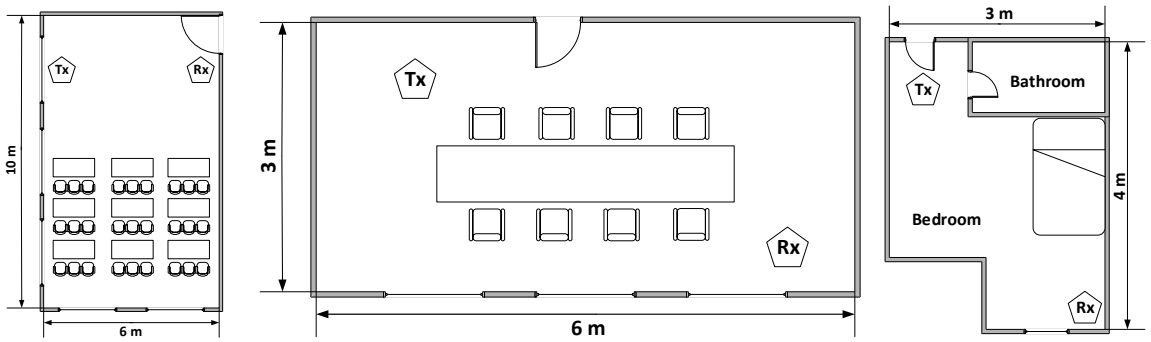

(a) Classroom (b) Meeting room (c) Dormitory room

Fig. 7 Floor plans.

how the sampling rate affects the performance of the proposed methodology.

In order to obtain the ground truth of environmental conditions, we place a 360 D600 camera, which has a wide-angle lens, around the receiver. The range of vision covers the monitoring area.

5.2 Performance

5.2.1 Evaluation metric

We use the following metrics to extensively evaluate the performance of our system and compare it with those of PADS[2] and FIMD[3].

• True Positive rate of human Movement Event (ME-TP). ME-TP is the probability that a human presence event is correctly detected.

• False Alarm (FA). FA is the number of false alarms of movement events when no human is actually present.

• True Positive and True Negative rates of human Movement Duration (denoted as MD-TP and MD-TN, respectively). MD-TP (MD-TN) calculates the overlapping time periods between detected movement (non-movement) events and ground truths.

• Errors of Movement Beginning (MBE) and Ending time (MEE). MBE and MEE are the delays (time biases with respect to ground truths) when an event is detected to start or end, respectively. A motion event's start means when a user begins to move in the monitoring area, and a motion event's end means when a user stops moving in the monitoring area.

5.2.2 Overall performance

With tiny WiFi nodes deployed in the meeting room for one day and in the dormitory room for two days, we evaluate the overall performance of WiSH. The results are shown in Table 1.

We observe that the ME-TP rate exceeds 98% in both scenarios. The MD-TP rate (duration accuracy) is relatively low compared with the ME-TP rate (event accuracy). It is rational if we take the speed of the moving target, sensitivity variety at different locations, and other factors into consideration, which are comprehensively discussed hereinafter. False alarms can be further minimized if we choose a channel that suffers less radio frequency interference as other devices may operate in the same channel.

Table 1 Overall performance of WiSH.

Scenario	ME-TP (%)	FA	MD-TP (%)	MD-TN (%)	MBE (s)	MEE (s)
Meeting room	98.83	4	81	91.45	1.46	2.95
Dormitory room	98.58	6	82	94.25	1.48	2.08

To evaluate the real-time performance of the system, we calculate the deviation of boundaries of movement events. Table 1 shows the average MBE and MEE in the two scenarios. The time delay of detecting whether a movement event starts (MBE) cannot be avoided because we utilize a time series to perform human detection robustly as illustrated in Section 3.3. However, we believe the delays are tolerable considering the average time span of movement events. Note that MEE is much larger than MBE. The rationale lies in that CSI cannot be static as soon as the target stops moving. Thus MD-TN cannot reach 100% as well. Figure 8 shows the distribution of MBE and MEE of 170 movement events that occur in the meeting room. The median deviation is 1.35 s for the beginning time and 1.07 s for the ending time. About 90% of motion events can be correctly detected with deviation less than 2.2 s. Note that MEE can be a negative value because micro movements might be discarded by the system.

We choose different numbers of selected subcarriers and employ the detection algorithm on 17 005 records to

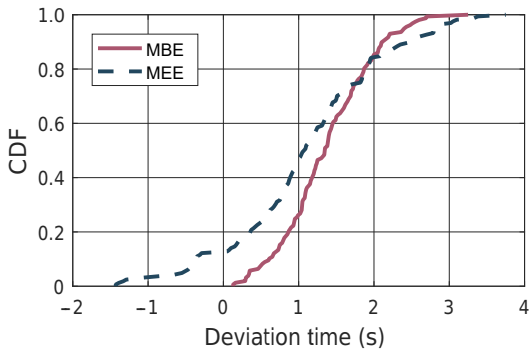

Fig. 8 Distribution of event boundary error. CDF represents cumulative distribution function.

prove the efficiency of our selection mechanism before calculating the cross-correlation in frequency domain. Table 2 shows that 45 selected subcarriers can guarantee ME-TP and the desired deviation time; simultaneously, the operation time is largely shortened.

We also operate FIMD[3] and PADS[2] on the tiny nodes to verify the low computational complexity of WiSH and compare their detection accuracy. The difference among the three systems is the methodology used to calculate the MI (see Section 3.2). WiSH utilizes the correlation of CSI amplitude in both time and frequency domains. FIMD uses only the time correlation of CSI amplitude, and it adopts a more sophisticated method, which calculates eigenvalues of the correlation matrix. PADS employs both amplitude and phase information to extract features, and it also performs eigenvalue decomposition. With CSI collected in 15 minutes as input, WiSH, FIMD, and PADS take 0.0145, 0.8911, and 1.7765 s, respectively, to calculate MI. Thus, PADS and FIMD cannot meet the requirements of real time if the system operates with a low sampling rate in one day. Figure 9 shows the distribution of the true positive rate of motion duration for 70 events. The performance of WiSH is comparable with that of FIMD in terms of duration accuracy. However, WiSH avoids complex calculations of eigenvalues and is more feasible for embedded devices, which have limited computational resources.

Table 2 Performance with different numbers of selected subcarriers.

Number of selected subcarriers	ME-TP (%)	FA	Deviation time (s)	Time cost (s)
90	98.75	0	1.63	2544.19
45	98.75	0	1.59	740.36
30	96.25	0	1.67	344.74

5.2.3 Parameter study

Now we study the impacts of different parameters on the system's performance.

Distance between transmitter and receiver. We conduct the experiments in a classroom. The distance between the transmitting node and receiving node varies from 2 m to 4 m. A volunteer is asked to walk evenly in a square area of 4 m × 6 m in which the nodes are placed. As Fig. 10 shows, when the distance decreases to 2 m, the ME-TP rate drops to below 90%. The main reason is that if the nodes are placed too close to each other, Line-Of-Sight (LOS) will surpass other paths. Human movements exert a low influence on CSI, and WiSH fails to report some events. Thus, we choose 4 m as the proper distance between the transmitter (Tx) and receiver (Rx) for other parameter studies.

Distance between human and LOS. In order to determine the effective covering range of WiSH with tiny nodes deployed, a volunteer is asked to walk along a route that is parallel with LOS. The vertical distance between the route and LOS changes from 0 to 3 m. As

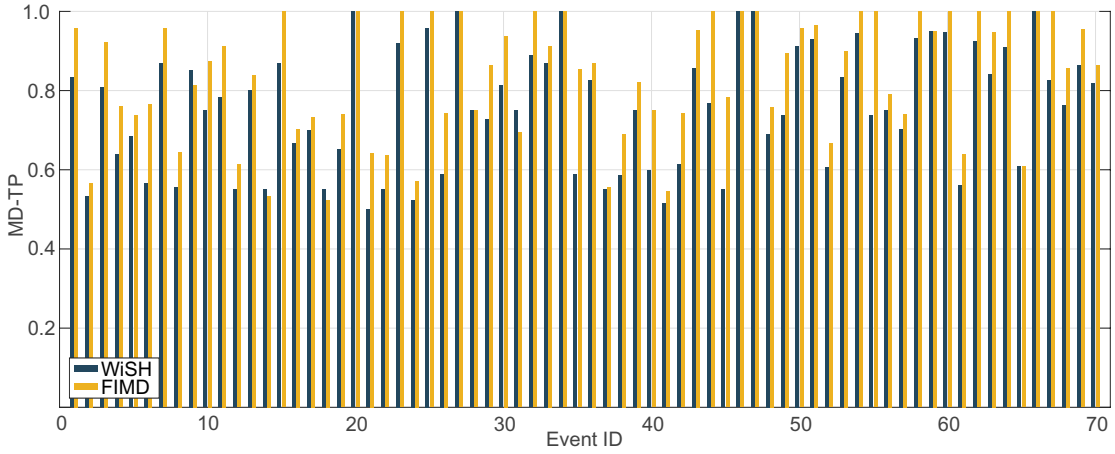

Fig. 9 Detection accuracy of WiSH and FIMD.

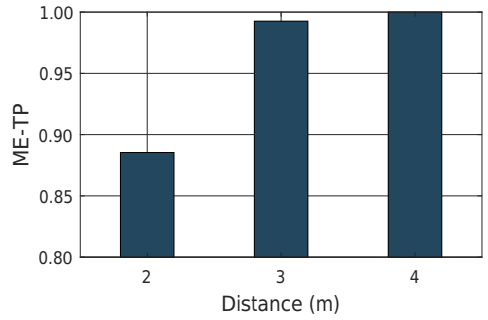

Fig. 10 Impact of distance between Tx and Rx.

the distance increases to 3 m, the ME-TP rate drops dramatically to around 58% as shown in Fig. 11. Thus, if the moving target is located too far away from the nodes, then WiSH may not work. However, we believe that this problem can be handled well if additional nodes are deployed in the classroom.

Distance between human and transmitter. If the moving event occurs at different locations, then CSI might suffer dynamics at various degrees. Therefore, we ask a volunteer to walk along a route that is perpendicular to LOS in order to validate the robustness of WiSH. The total length of the route is 6 m. As shown in Fig. 12, the ME-TP rate remains over 92% regardless of the distance between a human and transmitter. Thus, we believe such factor only exerts a slight influence on the performance of WiSH.

Moving speed. Fast human movements result in drastic changes in CSI amplitude in both time domain and frequency domains. However, the instantaneous velocity of slow movements is rather small, and moving events cannot be captured by simply employing the correlation property of CSI. With the robust filter proposed in Section 3.3, WiSH is capable of detecting slow movements effectively as well. As Fig. 13 illustrates, WiSH demonstrates high accuracy regardless of speed variations. Even if the moving target walks slowly in the monitoring area, the ME-TP rate exceeds 99%.

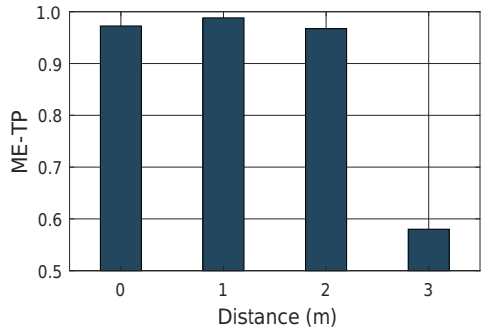

Fig. 11 Impact of distance between human and LOS.

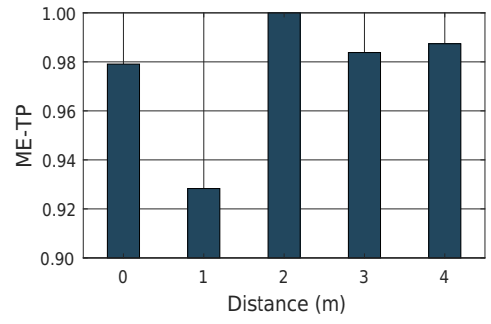

Fig. 12 Impact of distance between human and Tx.

Detection threshold. Intuitively, a large detection threshold will lead to increased sensitivity. As shown in Fig. 14a, ME-TP increases with rising detection threshold. However, when the detection threshold exceeds 0.98, some correlation values in static cases are below the threshold, so false alarms start to

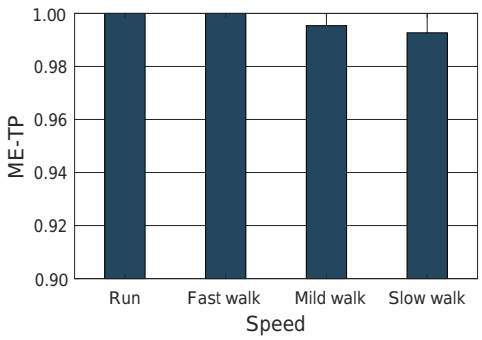

Fig. 13 Impact of moving speed.

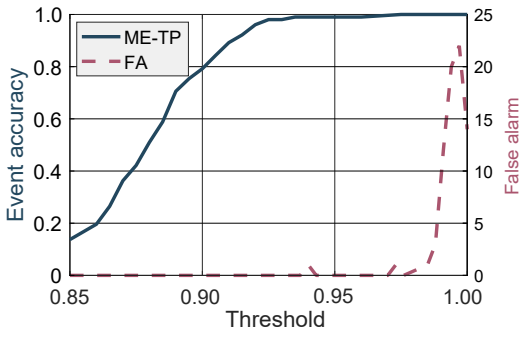

(a) Event detection and false alarm rate

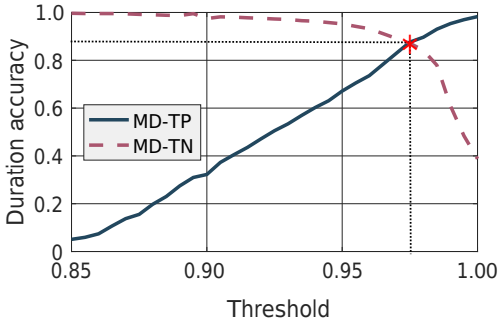

(b) ROC

Fig. 14 Impact of detection threshold.

increase. Figure 14b shows the change of duration accuracy against the detection threshold. Consistently, MD-TP increases and MD-TN decreases as the detection threshold increases. Although the balance point for duration accuracy is 0.975, we focus on a more accurate ME-TP and fewer false alarms. Thus, we choose 0.959 as the final detection threshold.

Sliding window size. Intuitively, the performance of WiSH will improve if the sliding window size is larger as the corresponding observation time is expanded. As shown in Fig. 15, ME-TP increases apparently when the window size rises to 2 s. However, when the window size is too large, ME-TP will decrease instead. This trend is reasonable because when the duration of human movements is very small, the corresponding dynamic CSI measurements only occupy a tiny proportion compared with the static period. Thus, the system will consider this case as a static one, and ME-TP falls.

Now we analyze how MD-TP is impacted by the sliding window size. When the window size decreases, the system will become more sensitive to human movements. Therefore, MD-TP increases as the window size decreases. Nevertheless, given that abrupt fluctuations in CSI occasionally occur, the overall performance will degrade when the window size is too small. Thus, a trade-off is necessary, and 1.2 s is regarded as a proper sliding window size.

Thresholds in the robust event filter. As mentioned in Section 3.3, we need to adopt two thresholds d_1 and d_2 for fewer false alarms and human movements missing. We refer to d_1 and d_2 as the minimum moving event duration and the minimum static event duration, respectively. As shown in Fig. 16a, d_1 exerts more influence on ME-TP than d_2. Moreover, false alarms decrease drastically when proper thresholds are selected (see Fig. 16b). To ensure both a high ME-TP rate and a small number of false alarms, we choose the minimum moving event duration as 1.1 s and the minimum static event duration as 1.1 s.

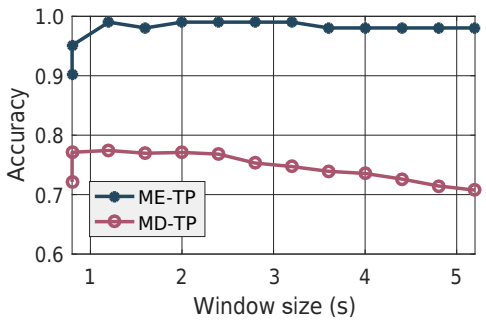

Fig. 15 Impact of window size.

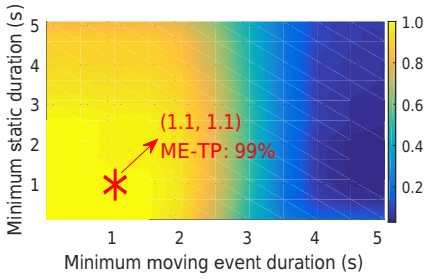

(a) Detection rate

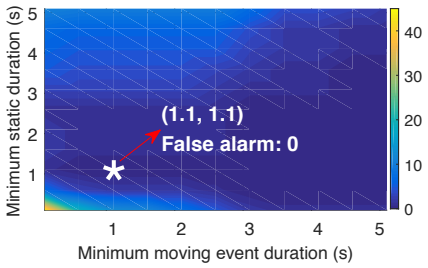

(b) False alarm

Fig. 16 Impact of minimum event length.

Sampling rate. Although we aim to enable accurate movement detection with low sampling rate limitation (less than 20 Hz) on our tiny nodes, we also evaluate and compare the performance under different sample rates. The experiments are conducted with the traditional wireless platform, which consists of a router and a mini desktop. As Fig. 17 shows, the MD-TN rate changes slightly with increasing sampling rate, but the ME-TP rate remains at 100%. As increasing sampling rate results in additional CSI measurements collected, the detection methodology will become more robust if the sliding window size does not vary. We observe that the ratio of detected duration correctly overlapping with true events increases from 76.7% to 92.5% when the sampling rate increases from 20 Hz to 90 Hz.

6 Related Work

6.1 RF-based passive moving human detection

Considering that vision-based human detection systems[18–20] function with strict constraints (e.g., LOS

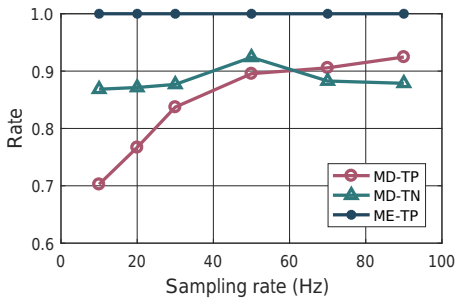

Fig. 17 Impact of sampling rate.

and lighting) and require heavy computing, researchers are devoted to finding alternatives. The concept of RF-based passive localization/detection originates in a previous work[21], which aims to localize or track a person without carrying any RF devices. To implement device-free systems, many prior works utilize RSSI, which can be obtained from WiFi devices[22], ZigBee nodes[23], and RFID readers[24,25]. The rationale lies in that the variance of RSSI increases when moving entities exist in the monitoring area. However, the performance of RSSI-based moving human detection algorithms might suffer from dramatic degradation[26] due to multipath effects and temporal dynamics.

Many research efforts have been devoted to CSI-based schemes because CSI can be exported from off-the-shelf NICs with slight driver modification[16]. Compared with RSSI, CSI provides both amplitude and phase information. It is also capable of discriminating multipath characteristics. Therefore, the system's performance can be largely improved by exploiting CSI. On the basis that the temporal correlation of CSI is much higher in static environment, Ref. [3] implements accurate fine-grained burst motion detection. Omni-PHD harnesses the histogram feature of the subcarrier amplitudes to implement omni-directional passive human detection[15]. PADS[2] is the first effort to leverage phase information in passive target detection. R-TTWD[27] proposes a subcarrier dimension-based feature to implement through-the-wall detection. RoMD[28] also takes the impacts of antenna selection into consideration. Most prior studies, however, still suffer from several limitations for real-time applications. Typically, they usually require prior training, extremely high sampling rates, and complex algorithms, which make them infeasible for energy-efficient and real-time applications. In this paper, we propose a lightweight system for real-time sensing of human detection. The system only requires a low sampling rate and can function on embedded devices with limited computational resources.

6.2 WiFi-based activity recognition

Apart from human presence detection, a large number of innovative applications and systems have emerged by exploiting WiFi, including localization[29–32], gesture recognition[5,33,34], gait recognition[6], smoking detection[7], sleep monitoring[9,35], fall detection[10], respiration and heart rate monitoring[11,36], etc. Recent works can be mainly divided into two categories. Some rely on location and environment-dependent features[4], such as CSI amplitude profiles. The recognition model needs to be re-trained for each different scenario. Others extract environment-independent features from original CSI, such as velocity[37,38] and Doppler shifts[33,39]. However, many works still adopt learning-based solutions and rely on rigorous requisites. Keystroke and activity recognition systems[4,8,13] use off-the-shelf WiFi devices, and they require extensive prior training at different locations in order to achieve high recognition accuracy. For accurate localization and tracking in Refs. [12, 37], dense links must be deployed preliminarily. Sleep and respiration monitoring systems[9,40] require users to be sufficiently close to the wireless links. Otherwise, the detection accuracy cannot be guaranteed. And most sensing applications only work in rather ideal environments without interference. In this paper, we design and implement a real-time passive human detection system that does not rely on rigorous requisites and works in practice. WiSH employs lightweight but effective methods and enables detection even on resource-limited devices with rather low sampling rates.

7 Conclusion

This paper presents the design and implementation of WiSH, a real-time human presence detection system for whole-day usage. Considering various practical constraints, we propose a lightweight yet effective detection method based on both time and frequency correlations of CSI measurements. To sift out CSI eruptions due to irrelevant instantaneous motions or environmental changes, we further design a robust event filter that identifies targeted human presence events. We implement WiSH on resource-limited RF devices and evaluate its performance in different scenarios. Results demonstrate that WiSH achieves a remarkable detection accuracy that exceeds 98%. With the sampling rate of 20 Hz, the average detection delay is merely 1.5 s and the durations of all detected events overlap with true events by 76.7%, which grows to 92.5% if the sampling rate increases to 90 Hz. We believe that WiSH is a practical system for real-time human detection in practice, and it can be deployed at large scale for long-term monitoring in real-world scenarios.

8 Future Work

In the monitoring rectangle area, we can obtain results with high accuracy around the LOS between sender and

receiver tiny nodes. However, if a human moves in the area far from this LOS, the system may not function because of long distance and low sampling rate. To solve this problem, we can deploy additional receiver nodes to cover the monitoring area as wide as possible. Furthermore, we can combine data collected by all receiver nodes together to achieve higher accuracy, but synchronizing all nodes is a major challenge.

In this study, we only use CSI amplitude in both time domain and frequency domains and have already achieved high accuracy. However, other parameters such as noise-signal ratio have not been utilized yet. Given that we need to find a balance between accuracy and operation time under limited computing environment, under the premise of short operation time, we may use other parameters in the future to improve our model and achieve increased accuracy.

Acknowledgment

This work was supported in part by the National Key Research Plan (No. 2016YFC0700100), the National Natural Science Foundation of China (Nos. 61832010, 61332004, and 61572366).

References

[1] Z. M. Zhou, C. S. Wu, Z. Yang, and Y. H. Liu, Sensorless sensing with WiFi, *Tsinghua Sci. Technol.*, vol. 20, no. 1, pp. 1–6, 2015.

[2] K. Qian, C. S. Wu, Z. Yang, Y. H. Liu, and Z. M. Zhou, PADS: Passive detection of moving targets with dynamic speed using PHY layer information, in *Proc. 20th IEEE Int. Conf. Parallel and Distributed Systems*, Hsinchu, China, 2014.

[3] J. Xiao, K. S. Wu, Y. W. Yi, L. Wang, and L. M. Ni, FIMD: Fine-grained device-free motion detection, in *Proc. 18th Int. Conf. Parallel and Distributed Systems*, Singapore, 2012.

[4] Y. Wang, J. Liu, Y. Y. Chen, M. Gruteser, J. Yang, and H. B. Liu, E-eyes: Device-free location-oriented activity identification using fine-grained WiFi signatures, in *Proc. 20th Annu. Int. Conf. Mobile Computing and Networking*, Maui, HI, USA, 2014.

[5] Q. F. Pu, S. Gupta, S. Gollakota, and S. Patel, Whole-home gesture recognition using wireless signals, in *Proc. 19th Annu. Int. Conf. Mobile Computing & Networking*, Miami, FL, USA, 2013.

[6] W. Wang, A. X. Liu, and M. Shahzad, Gait recognition using WiFi signals, in *Proc. ACM Int. Joint Conf. Pervasive and Ubiquitous Computing*, Heidelberg, Germany, 2016.

[7] X. L. Zheng, J. L. Wang, L. F. Shangguan, Z. M. Zhou, and Y. H. Liu, Smokey: Ubiquitous smoking detection with commercial WiFi infrastructures, in *Proc. 35th Annu. IEEE Int. Conf. Computer Communications*, San Francisco, CA, USA, 2016.

[8] M. Y. Li, Y. Meng, J. Y. Liu, H. J. Zhu, X. H. Liang, Y. Liu, and N. Ruan, When CSI meets public WiFi: Inferring your mobile phone password via WiFi signals, in *Proc. 2016 ACM SIGSAC Conf. Computer and Communications Security*, Vienna, Austria, 2016.

[9] X. F. Liu, J. N. Cao, S. J. Tang, and J. Q. Wen, Wi-sleep: Contactless sleep monitoring via WiFi signals, in *Proc. IEEE Real-Time Systems Symp.*, Rome, Italy, 2014.

[10] H. Wang, D. Q. Zhang, Y. S. Wang, J. Y. Ma, Y. X. Wang, and S. J. Li, RT-fall: A real-time and contactless fall detection system with commodity WiFi devices, *IEEE Trans. Mobile Comput.*, vol. 16, no. 2, pp. 511–526, 2017.

[11] J. Liu, Y. Wang, Y. Y. Chen, J. Yang, X. Chen, and J. Cheng, Tracking vital signs during sleep leveraging off-the-shelf WiFi, in *Proc. 16th ACM Int. Symp. Mobile Ad Hoc Networking and Computing*, Hangzhou, China, 2015.

[12] J. Wang, H. B. Jiang, J. Xiong, K. Jamieson, X. J. Chen, D. Y. Fang, and B. B. Xie, LiFS: Low human-effort, device-free localization with fine-grained subcarrier information, in *Proc. 22nd Annu. Int. Conf. Mobile Computing and Networking*, New York, NY, USA, 2016.

[13] B. Wei, W. Hu, M. R. Yang, and C. T. Chou, Radio-based device-free activity recognition with radio frequency interference, in *Proc. 14th Int. Conf. Information Processing in Sensor Networks*, Seattle, WA, USA, 2015.

[14] C. S. Wu, Z. Yang, Z. M. Zhou, X. F. Liu, Y. H. Liu, and J. N. Cao, Non-invasive detection of moving and stationary human with WiFi, *IEEE J. Sel. Areas Commun.*, vol. 33, no. 11, pp. 2329–2342, 2015.

[15] Z. M. Zhou, Z. Yang, C. S. Wu, L. F. Shangguan, and Y. H. Liu, Towards omnidirectional passive human detection, in *Proc. IEEE INFOCOM*, Turin, Italy, 2013.

[16] D. Halperin, W. J. Hu, A. Sheth, and D. Wetherall, Predictable 802.11 packet delivery from wireless channel measurements, in *Proc. ACM SIGCOMM 2010 Conf.*, New Delhi, India, 2010.

[17] Y. X. Xie, Z. J. Li, and M. Li, Precise power delay profiling with commodity WiFi, in *Proc. 21st Annu. Int. Conf. Mobile Computing and Networking*, Paris, France, 2015.

[18] N. Dalal, B. Triggs, and C. Schmid, Human detection using oriented histograms of flow and appearance, in *Proc. 9th European Conf. Computer Vision*, Graz, Austria, 2006.

[19] L. Xia, C. C. Chen, and J. K. Aggarwal, Human detection using depth information by Kinect, in *Proc. CVPR 2011 WORKSHOPS*, Colorado Springs, CO, USA, 2011.

[20] C. H. Morimoto, D. Koons, A. Amir, and M. Flickner, Pupil detection and tracking using multiple light sources, *Image Vis. Comput.*, vol. 18, no. 4, pp. 331–335, 2000.

[21] M. Youssef, M. Mah, and A. Agrawala, Challenges: Device-free passive localization for wireless environments, in *Proc. 13th Annu. ACM Int. Conf. Mobile Computing and Networking*, Montreal, Canada, 2007.

[22] A. E. Kosba, A. Saeed, and M. Youssef, RASID: A robust WLAN device-free passive motion detection system, in *Proc. 2012 IEEE Int. Conf. Pervasive Computing and Communications*, Lugano, Switzerland, 2012.

[23] D. Zhang, J. Ma, Q. B. Chen, and L. M. Ni, An RF-based system for tracking transceiver-free objects, in *Proc.*

5th Annu. IEEE Int. Conf. Pervasive Computing and Communications, White Plains, NY, USA, 2007.

[24] J. S. Han, C. Qian, X. Wang, D. Ma, J. Z. Zhao, P. F. Zhang, W. Xi, and Z. P. Jiang, Twins: Device-free object tracking using passive tags, in *Proc. 33rd Annu. IEEE Conf. Computer Communications*, Toronto, Canada, 2014.

[25] L. F. Shangguan, Z. Yang, A. X. Liu, Z. M. Zhou, and Y. H. Liu, STPP: Spatial-temporal phase profiling-based method for relative RFID tag localization, *IEEE/ACM Trans. Netw.*, vol. 25, no. 1, pp. 596–609, 2017.

[26] Z. Yang, Z. M. Zhou, and Y. H. Liu, From RSSI to CSI: Indoor localization via channel response, *ACM Comput. Surv.*, vol. 46, no. 2, p. 25, 2013.

[27] H. Zhu, F. Xiao, L. J. Sun, R. C. Wang, and P. L. Yang, R-TTWD: Robust device-free through-the-wall detection of moving human with WiFi, *IEEE J. Sel. Areas Commun*, vol. 35, no. 5, pp. 1090–1103, 2017.

[28] G. Liu, Y. L. Li, D. Li, X. L. Ma, and F. M. Li, RoMD: Robust device-free motion detection usin PHY layer information, in *Proc. 12th Annu. IEEE Int. Conf. Sensing, Communication, and Networking*, Seattle, WA, USA, 2015.

[29] C. S. Wu, Z. Yang, and Y. H. Liu, Smartphones based crowdsourcing for indoor localization, in *IEEE Trans. Mobile Comput.*, vol. 14, no. 2, pp. 444–457, 2015.

[30] Z. Yang, C. S. Wu, Z. M. Zhou, X. L. Zhang, X. Wang, and Y. H. Liu, Mobility increases localizability: A survey on wireless indoor localization using inertial sensors, *ACM Comput. Surv.*, vol. 47, no. 3, p. 54, 2015.

[31] C. S. Wu, Z. Yang, and C. W. Xiao, Automatic radio map adaptation for indoor localization using smartphones, *IEEE Trans. Mobile Comput.*, vol. 17, no. 3, pp. 517–528, 2018.

[32] Z. W. Yin, C. S. Wu, Z. Yang, and Y. H. Liu, Peer-to-peer indoor navigation using smartphones, *IEEE J. Sel. Areas Commun.*, vol. 35, no. 5, pp. 1141–1153, 2017.

[33] K. Qian, C. S. Wu, Z. M. Zhou, Y. Zheng, Z. Yang, and Y. H. Liu, Inferring motion direction using commodity Wi-Fi for interactive exergames, in *Proc. ACM CHI Conf. Human Factors in Computing Systems*, Denver, CO, USA, 2017.

[34] A. Virmani and M. Shahzad, Position and orientation agnostic gesture recognition using WiFi, in *Proc. 15th Annu. Int. Conf. Mobile Systems, Applications, and Services*, Niagara Falls, NY, USA, 2017.

[35] C. Y. Hsu, A. Ahuja, S. C. Yue, R. Hristov, Z. Kabelac, and D. Katabi, Zero-effort in-home sleep and insomnia monitoring using radio signals, in *Proc. ACM on Interactive, Mobile, Wearable and Ubiquitous Technologies*, New York, NY, USA, 2017.

[36] F. Adib, H. Z. Mao, Z. Kabelac, D. Katabi, and R. C. Miller, Smart homes that monitor breathing and heart rate, in *Proc. 33rd Annu. ACM Conf. Human Factors in Computing Systems*, Seoul, Republic of Korea, 2015.

[37] K. Qian, C. S. Wu, Z. Yang, Y. H. Liu, and K. Jamieson, Widar: Decimeter-level passive tracking via velocity monitoring with commodity Wi-Fi, in *Proc. 18th ACM Int. Symp. Mobile Ad Hoc Networking and Computing*, Chennai, India, 2017.

[38] W. Wang, A. X. Liu, M. Shahzad, K. Ling, and S. L. Lu, Understanding and modeling of WiFi signal based human activity recognition, in *Proc. 21st Annu. Int. Conf. Mobile Computing and Networking*, Paris, France, 2015.

[39] K. Qian, C. S. Wu, Y. Zhang, G. D. Zhang, Z. Yang, and Y. H. Liu, Widar2.0: Passive human tracking with a single Wi-Fi link, in *Proc. 16th Annu. Int. Conf. Mobile Systems, Applications, and Services*, Munich, Germany, 2018.

[40] H. Wang, D. Q. Zhang, J. Y. Ma, Y. S. Wang, Y. X. Wang, D. Wu, T. Gu, and B. Xie, Human respiration detection with commodity WiFi devices: Do user location and body orientation matter? in *Proc. 2016 ACM Int. Joint Conf. Pervasive and Ubiquitous Computing*, Heidelberg, Germany, 2016.

Tianmeng Hang received the BEng degree from Beijing University of Posts and Telecommunications in 2015, and the MEng degree from Tsinghua University in 2018. Her research interests include wireless networks and mobile computing.

Yue Zheng received the BEng degree from Tsinghua University, China, in 2015. She is currently a PhD student in Department of Electronic Engineering and School of Software at Tsinghua University. She is a member of the Beijing National Research Center for Information Science and Technology. Her research interests include wireless networks and mobile computing.

Kun Qian received the BEng degree from Tsinghua University in 2014. He is currently working toward the PhD degree in the School of Software, Tsinghua University. He is a member of the Beijing National Research Center for Information Science and Technology. His research interests include wireless networks and mobile computing.

Chenshu Wu received the BEng and PhD degrees from Tsinghua University in 2010 and 2015, respectively. He is currently with the Department of Electrical and Computer Engineering, University of Maryland, College Park, MD, USA. His research interests include wireless networks and mobile computing.

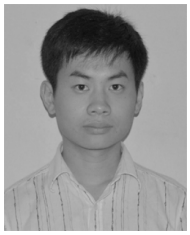

Zheng Yang received the BEng degree from Tsinghua University in 2006, and the PhD degree from Hong Kong University of Science and Technology in 2010. He is currently an associate professor with Tsinghua University. His main research interests include wireless ad-hoc/sensor networks and mobile computing.

Yunhao Liu received the BS degree from Tsinghua University in 1995, and the MS and PhD degrees from Michigan State University in 2003 and 2004, respectively. He is now the foundation professor and chairperson of Department of Computer Science and Engineering, Michigan State University, and holds Chang Jiang Chair Professorship (No Pay Leave) at Tsinghua University. His research interests include wireless sensor network, peer-to-peer computing, and pervasive computing.

Xiancun Zhou received the BS degree from Anhui University, China, in 1997, and received the MS degree from Heifei University of Technology in 2004. She is now a professor at the Department of Information Engineering in West Anhui University. Her current research interests include information security and wireless networks.

Guilin Chen received the BS degree from Anhui Normal University in 1985, and received the MS degree from Heifei University of Technology in 2002. He is now a professor at the School of Computer Science and Information Engineering in Chuzhou University. His current research interests include Internet of things.